ORIGINAL ARTICLE

INTESTINAL RESEARCH

pISSN 1598-9100 • eISSN 2288-1956
https://doi.org/10.5217/ir.2018.16.1.116
Intest Res 2018;16(1):116-125

Topographic, histological and molecular study of aberrant crypt foci identified in human colon in different clinical groups

Shouriyo Ghosh[1], Brijnandan Gupta[1], Pavan Verma[1], Sreenivas Vishnubathla[2], Sujoy Pal[3], Nihar R Dash[3], Siddhartha Datta Gupta[1], Prasenjit Das[1]

Departments of [1]Pathology, [2]Biostatistics, and [3]Gastrointestinal Surgery, All India Institute of Medical Sciences, New Delhi, India

Background/Aims: Aberrant crypt foci (ACF) are early microscopic lesions of the colonic mucosa, which can be detected by magnified chromoendoscopy. Herein, we have investigated whether ACF identified in different clinical groups can be differentiated based on their characteristics. **Methods:** Macroscopically unremarkable mucosal flaps were collected from 270 fresh colectomies and divided into 3 clinical groups: colorectal carcinoma (group A), disease controls having known pre-neoplastic potential (group Bc), and disease controls without risk of carcinoma development (group Bn). Topographic and histologic analysis, immunohistochemistry, and molecular studies (high-resolution melt curve analysis, real-time polymerase chain reaction, and Sanger sequencing) were conducted for certain neoplasia-associated markers. **Results:** ACF were seen in 107 cases, out of which 72 were left colonic ACF and 35 right colonic ACF (67.2% vs. 32.7%, *P*=0.02). The overall density of left colonic ACF was 0.97/cm, which was greater than the right colonic ACF density of 0.81/cm. Hypercrinia was present in 41 out of 72 left colonic ACF and in 14 out of 35 right colonic ACF (*P*=0.01). Immunohistochemical expression of p53 was also greater in left colonic ACF than in right colonic ACF (60.5% vs. 38.2%, *P*=0.03). However, ACF identified among the 3 clinical groups did not show any distinguishing topographic, histological, or genetic changes. **Conclusions:** Left colonic ACF appear to be high-risk based on their morphological and prototypic tumor marker signature. ACF identified in different clinical groups do not show significant genotypic or topographic differences. Further detailed genetic studies are required to elucidate them further. **(Intest Res 2018;16:116-125)**

Key Words: Aberrant crypt foci; Chromoendoscopy; *KRAS*; *BRAF*; *MMR*

INTRODUCTION

As Westernized dietary habits and urban lifestyles become more commonly embraced, the incidence of colorectal carcinoma (CRC) is expected to spike in the near future. At present, though the age adjusted incidence rate of CRC is still low in developing countries, the lack of awareness and affordable healthcare facilities result in detection of the disease at an already advanced stage.[1,2] Overall, CRC is one of the most common causes of cancer-related mortality worldwide.[3] Thus, it is necessary to introduce effective population-based screening programs, especially in developing nations where such programs do not exist. However, one of the drawbacks of conventional colonoscopic screening is that it can only detect macroscopic mucosal lesions, such as adenomas, when the lesion has already undergone complex genetic changes. Hence, future screening techniques should aim to detect early microscopic preneoplastic lesions before the development of mass lesions has occurred. Currently, narrow band imaging, confocal endoscopes, and chromoendoscopy are increasingly available in major cities, which may

Received May 7, 2017. **Revised** September 23, 2017.
Accepted September 27, 2017. **Published online** November 24, 2017
Correspondence to Prasenjit Das, Department of Pathology, All India Institute of Medical Sciences, Room No. 3093, 3rd Floor, Teaching Block, New Delhi 110029, India. Tel: +91-11-26594979, Fax: +91-11-26588663 / 26588641, E-mail: prasenaiims@gmail.com

enable the *in vivo* detection of microscopic preneoplastic lesions, such as aberrant crypt foci (ACF).[4]

ACF-like lesions were first identified during the microscopic examination of mutagen treated colonic mucosa in rodents and were subsequently identified in human colonic mucosae.[5-8] In a recently published study, we demonstrated the up-regulation of cancer stem cell (CSC) marker CD24 in ACF, similar to that in CRC, in comparison to that in the normal colon.[9] Kudo et al.[10] also showed the up-regulation of CSC marker LGR-5 in the ACF of mutagen-treated mice. Despite these interesting findings, the lack of a comprehensive understanding of the ACF-like lesions in human colon has not led to the clinical use of these lesions as markers of early disease in the human colonic mucosa. It remains unclear whether all ACF-like lesions in the human colon are potentially malignant, or if a specific morphological, topographic, or genetic subgroup is more prone to malignant change. In our previous study, we observed that ACF-like lesions could be identified in a wide variety of colectomy specimens from patients undergoing surgery because of various indications.[9] In this study, we sought to examine whether topographic, histological, and genetic changes differ in ACF identified in different clinical groups and also to identify the characteristics of high-risk ACF in the human colon.

METHODS

1. Patients Characteristics and Sample Preparation

This was a cross-sectional study conducted on a total of 270 fresh colorectal resection specimens, irrespective of the indication for surgery. Among these 270 specimens, ACF were identified in 107 specimens. Cases with a history of neoadjuvant therapy were excluded. The colectomy specimens with ACF were divided into following 3 clinical groups. Group A included colectomies performed for CRC (n=67). Group B (n=40) contained the disease controls and were further subdivided into group Bc (n=23; colectomies performed for conditions with an established link of colonic carcinoma development; e.g., 19 surgeries performed for chronic IBD of more than 10 years' duration, 4 adenomatous polyposis, etc.) and group Bn (n=17; colectomies performed for diseases having no known link with any neoplastic lesion development, e.g., 7 ischemic bowel disease, 3 tuberculosis, 2 intestinal perforation, 4 Hirschsprung disease, and 1 gastric gastrointestinal stromal tumor).

After receiving the fresh specimens, macroscopically normal-looking colonic mucosa situated at least 10 cm away from the tumor was identified and dissected out from the underlying submucosa. For all specimens, the shaved mucosal flap size as 2.5 cm×2.5 cm with an area of approximately 6.25 cm^2. These mucosal flaps were then stretched out on a paraffinized plate and fixed overnight in 10% neutral buffered formalin. In the non-tumor group, mucosal flaps were randomly sampled.

2. Identification and Immunohistochemistry of ACF

Following fixation, these flaps were stained with 0.5% methylene blue and observed for ACF at low-power magnification (×40 magnification) under an Olympus BX50 microscope (Tokyo, Japan). Single crypts or groups of distorted and darkly stained crypts were marked with water-resistant tissue paint (Davidson Marking System; Bradley Product, Inc., Bloomington, MN, USA). During the gross identification of ACF, various parameters such as elevation of the ACF, Kudo's pit pattern,[10] crypt pattern according to our previous descriptions, size, frequency, and multiplicity of the ACF were assessed and recorded.[9] Each case was photographed at ×40 magnification for computer-assisted image analysis. The marked areas of the flaps were then cut into thin strips and processed for paraffin embedding to confirm the ACF by H&E staining. Histological confirmation of ACF, along with mucosal histology, the presence or absence of dysplasia, and hypercrinia were noted by 2 pathologists independently. Cases with ACF confirmed on histology were then selected for the next part of the analysis. The subsequent part of analysis involved immunohistochemistry (IHC) and PCR for *KRAS* and *BRAFV600E* mutation detection. For molecular analysis, the blocks were stored separately in waterproof containers at 4°C.

IHC markers studied on the ACF-positive tissue sections included: (1) mismatch repair (*MMR*) protein markers, MLH1, MSH2, PMS2, MSH6; and (2) marker of cell cycle regulation, p53. Tissue sections (5 μm) were cut from the paraffin blocks and deparaffinized. Endogenous peroxidase was blocked using 4% hydrogen peroxide, followed by antigen retrieval through boiling in citrate buffer. Primary monoclonal antibodies for MLH1 (1:400; Bio SB, Santa Barbara, CA, USA), PMS2 (1:200; Spring Bioscience Corp., Pleasanton, CA, USA), MSH2 (1:200, Bio SB), MSH6 (1:100, Bio SB), and p53 (1:400, Spring Bioscience) were applied on the sections, and the slides were incubated overnight at 4°C. The reaction product was developed with 3,3'-diaminobenzidine and counterstained with hematoxylin. Appropriate positive and negative controls were used. The IHC slides

were then evaluated by comparing the staining pattern in the ACF with that in the adjacent normal-appearing crypts. IHC for MMR proteins was considered a surrogate marker for assessing microsatellite instability (MSI). Positive staining denoted functional expression of the gene product, and implied microsatellite stability. Any staining >10% of the epithelial cell nuclei was considered positive, i.e., microsatellite stable (MSS); staining in <10% of cells or negative staining was considered to represent MSI. p53 positivity in >10% of tumor cell nuclei was considered positive and to represent the surrogate marker for *TP53* mutation.[11] Expression of all the markers was noted separately in the ACF, tumors, and normal crypts.

3. Identification of *KRAS* and *BRAF* Mutations

KRAS mutation was tested in a total of 36 cases of ACF: CRC-associated ACF (n=26), ACF associated with control group Bc (n=4), and ACF associated with control group Bn (n=6). The cases were chosen based on presence of numerous ACF (>10 ACF/mm^2) in the colonic mucosa. The representative areas were then microdissected out from unstained 10-μm sections (for a total of approximately 50 μg) and placed in lysing buffer until proper tissue homogenization occurred. Subsequent steps involved precipitating DNA with the help of a binding buffer (Purelink Genomic DNA Mini Kit, Life Technologies, Carlsbad, CA, USA), repeated washing in the buffers provided, and then elution using micro-column-based technique. The DNA content and quality were measured using a NanoDrop machine. Mutation-specific forward and reverse primers (5'-GAATATAAACTTGTGGTAGTTGGAGCT-3' [F] and 5'-ATCGTCAAGGCACTCTTGCCTAC-3' [R]) were used to target codons 12 and 13 of the *KRAS* gene and their flanking regions, with a calculated amplicon size of 56 bp. DNA extracted from the blood of normal subjects was used as a negative control (wild-type *KRAS*). We performed high-resolution melting curve analysis using an AriaMX real-time PCR (qPCR) machine from Agilent Technologies (Santa Clara, CA, USA). The high-resolution melting curve analysis results were then validated by forward-strand sequencing in 10 representative samples (including the blood sample). For this part of the analysis, a separate primer was used to yield an amplicon of 254 base pairs, covering exon 2 of the *KRAS* gene. This amplicon was run by gel electrophoresis, eluted, and sequenced by Sanger sequencing. The results were analyzed using sequencing software by Applied Biosystems (Foster City, CA, USA).

BRAF mutation analysis was performed on 25 randomly selected cases from all 3 study groups. Extracted DNA was subjected to qPCR using *BRAF V600E*-specific probes, as described in an earlier study.[12] Briefly, a 25-μL reaction was prepared using a Taqman PCR core reagent kit (Applied Biosystems) and 900-nM forward and reverse primers, 250 nM of a wild-type probe, and a mutation-specific probe. The Taqman-MGB probes were specific for the *V600E* mutation (c.1799T>A) in BRAF exon 15. qPCR was performed using a Qiagen Rotor Gene-Q machine with the following conditions: 96°C for 10 minutes, 40 cycles of 96°C for 15 seconds, and 60°C for 30 seconds with acquisition in carboxyfluorescein (FAM) (for mutation) and VIC fluorescent dye (for wild-type) channels. Analysis and mutation calls were made using Rotor Gene Q software.

4. Statistical Analysis

Data analysis was performed using Stata 12.1 software (College Station, TX, USA). Mean ACF number and density were compared between the study groups using Kruskal-Wallis ANOVA. ACF density with laterality was analyzed using the Student *t*-test. ACF histology was analyzed in relation to the groups using the Fisher exact test. Association of hypercrinia with the study groups was performed using chi-square test. To evaluate the association of hypercrinia with laterality and ACF number simultaneously, the linear trend chi-square test was used. Analysis of Kudo et al.'s results[10] and those of our group using various parameters like laterality, ACF histology, and presence of hypercrinia was performed using the chi-square test. Similarly, all the IHC markers and mutation results were analyzed in relation to groups and parameters using the chi-square and linear trend chi-square tests. The study protocol was approved by the Institutional Review Board at the All India Institute of Medical Sciences, New Delhi, India (IRB numbers: IESC/T-34/03.01.2014, OT-3/30.09.2015) and performed in accordance with the principles of the Declaration of Helsinki. Informed consent was waived.

RESULTS

1. Basic Patient Data

Among the total of 270 mucosal flaps that were examined, ACF were identified in 107 (39.6%), including 67 colectomies performed for CRC (group A) and 40 colectomy cases from control group (group B). The patients (n=107) in whom ACF were identified included 69 men (age range, 7–84

https://doi.org/10.5217/ir.2018.16.1.116 • Intest Res 2018;16(1):116-125

Table 1. Comparing the Topographic and Histological Parameters in ACF Identified in 3 Clinical Groups

Parameter	ACF in control group Bn[a] (n=17)	ACF in controls group Bc[b] (n=23)	ACF in CRC cases (group A) (n=67)	*P*-value
ACF no.	4.58±1.40	3.86±1.20	5.32±1.90	0.34
ACF density (cm^2)	0.84±0.63	0.74±0.76	1.01±0.86	0.32
Presence of hypercrinia (%)	35.3	56.5	53.7	0.34
ACF morphology				0.23
ACF associated with normal mucosa	13 (76.5)	14 (60.9)	39 (58.2)	
ACF associated with hyperplastic mucosa	4 (23.5)	9 (39.1)	20 (29.9)	
ACF associated with dysplastic mucosa	0	0	8 (11.9)	

Values are presented as mean±SD or number (%).
[a]Bn, controls in which colectomy was performed for indications that do not have any association with colon carcinogenesis.
[b]Bc, controls in which colectomy was performed for indications that have a known association with colon carcinogenesis.
ACF, aberrant crypt foci.

years) and 38 women (age range, 11–71 years). There were 35 right hemicolectomy cases, whereas there were 72 left colectomies (abdominoperineal resections and low anterior resections).

2. Gross and Histologic Findings

All ACF identified directly on methylene blue-stained colonic mucosa under 40× magnification were subsequently confirmed through histological examination. The mean ACF number was calculated by adding the number of ACF in all cases in a group, with respect to the total number of cases in that particular group. The mean ACF number was greater in study group A (5.32, n=67/107) than in the control groups (group Bc: 3.86, n=23/107; group Bn: 4.58, n=17/107). However, the difference was not statistically significant (*P*=0.34) (Table 1). ACF density was also greater in cases of CRC (1.01/cm^2) than in groups Bc (0.74/cm^2) and Bn (0.84/cm^2); however, the difference was not statistically significant (*P*=0.32) (Table 1). ACF size (mean diameter) and the crypt multiplicity (number of single aberrant crypts coalescing to form an ACF) were also found to increase progressively across the groups, with the smallest size and lowest multiplicity noted in group Bc, intermediate size and multiplicity noted in group Bn, and the greatest size and highest multiplicity noted in group A. ACF number, density, and size, as well as crypt multiplicity, were greater on the left side of colon. Hypercrinia was found to increase as the number of ACF increased, especially in the left colon (*P*=0.02) (Table 2). Hypercrinia occurred more frequently in the left colon than in the right colon (72% vs. 35%, *P*=0.01). When evaluating the elevated or flat lesions with respect to location, we found more frequently elevated ACF in the left colonic mucosa (45/58, 77.5%) than in the right (13/58, 22.4%) (*P*=0.01). Out of the 107 ACF included, hyperplastic stratified mucosal lining in the foci of the ACF was noted in 30.8% of cases, with normal unilinear mucosal lining in 61.7% and dysplastic epithelial lining in 7.4% (Fig. 1D and E). Among the latter, low-grade dysplasia was noted in 7 of 107 (6.5%), whereas high-grade dysplasia was found in 1 of 107 (0.9%) of the aberrant crypts. All the dysplastic ACF were situated in the left colon. Hypercrinia was also identified in these left colonic dysplastic ACF (Fig. 1F). However, the single case of ACF with high-grade dysplasia had a paucity of mucin-secreting cells in the lining of the epithelium. There was no microscopic difference between elevated and flat ACF. Multiple ACF identified in one case (i.e., ACF located in the vicinity of each other in a single mucosal flap) shared nearly similar mucosal histol-

Table 2. Comparison of ACF Number with Hypercrinia and Laterality

Parameter	Presence of hypercrinia (in red)		*P*-value (hypercrinia)
	Right colon	Left colon	
ACF no.			0.01
1	2/7 (28.5)	5/14 (35.7)	
2	1/8 (12.5)	10/17 (58.8)	
3	1/4 (25.0)	3/5 (60.0)	
4	3/6 (50.0)	3/5 (60.0)	
≥5	7/10 (70.0)	20/31 (64.5)	
Total	35	72	
P-value (ACF no.)	0.02		

Values are presented as number/number (%).
ACF, aberrant crypt foci.

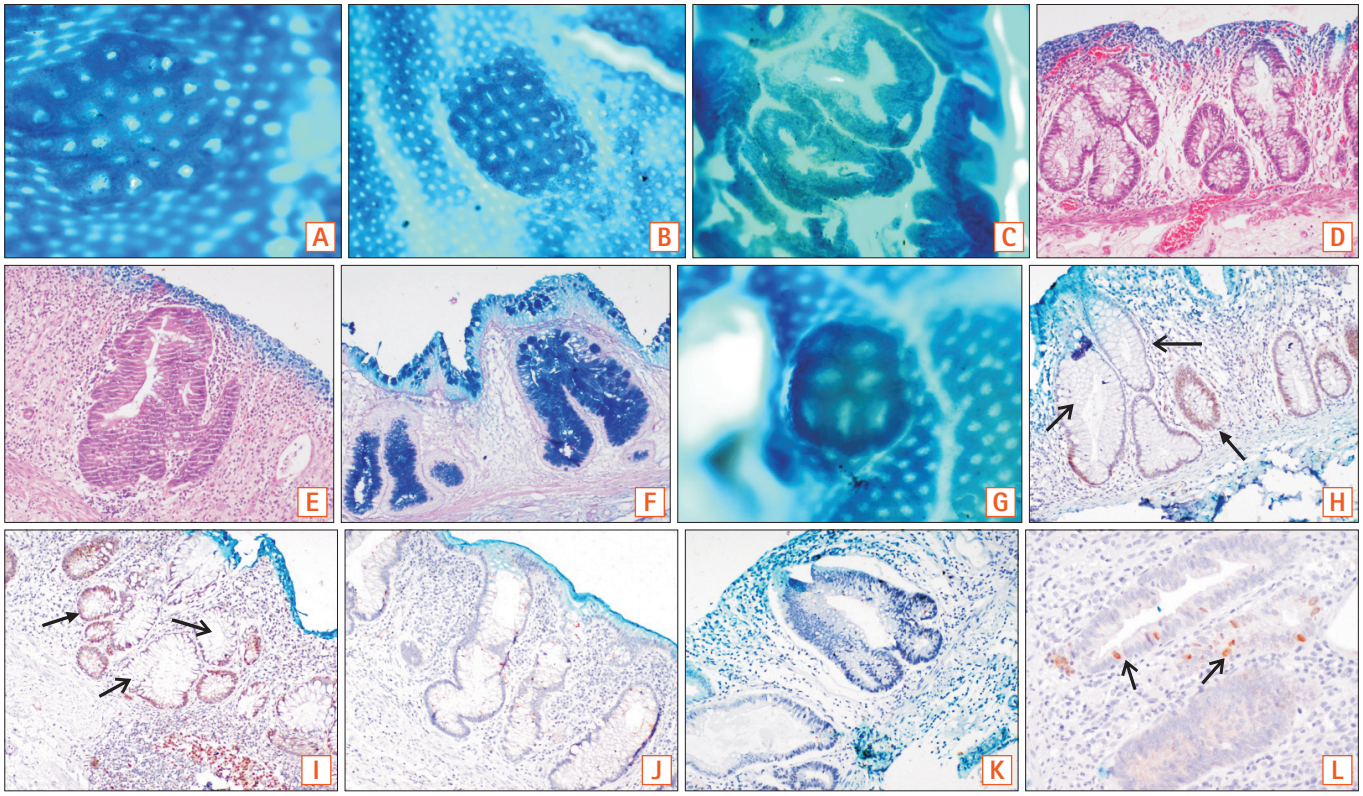

Fig. 1. Photographs showing aberrant crypt foci (ACF) with round pits (A), slit-like pits (B), and gyriform pits (C) (mucosa stained with methylene blue, ×40). ACF showing both hyperplastic (D, ×100) and dysplastic mucosal lining (E, ×100) (H&E). Hypercrinia ACF with numerous goblet cells and sparse absorptive cells (F, Alcian blue, ×100). Elevated ACF (G). Loss of nuclear MLH1 (H, ×100) and MSH2 stains (I, ×100), as seen in ACF (open head arrows), in comparison to that in normal crypts (closed head arrows) (immunohistochemistry). ACF with a complete loss of MSH6 (J, ×100) and PMS2 staining (K, ×100) and strong focal nuclear positivity (open head arrows) for p53 protein (L, ×100) (immunohistochemistry).

ogy and topographical characteristics. Accounting for a possible field effect of these closely situated mucosal lesions, we sampled all ACF from a particular case for further IHC and molecular analysis.

3. ACF Pit Pattern Analysis

We tried to classify the ACF pit patterns according to both the 6-tier classification system described by Kudo et al.[10] and to our customized 3-tier ACF-specific classification system: round (pattern 1), slit-like (pattern 2), and gyriform (pattern 3) (Fig. 1A-C).[9] We found a good correlation between Kudo's pattern 1 and our pattern 1, as both denoted round pits. Kudo's pattern 2, i.e., stellate or papillary pits, however, was distributed between our patterns 2 and 3. ACF with our pattern 3 were associated with a 17% rate of dysplasia, in comparison to 10% in pattern 2 and 5% in pattern 1. When Kudo's classification was applied to the index cases of ACF, we did not identify any linearity of Kudo's patterns with the rate of dysplasia (Kudo's pit pattern distribution in index cases: pattern 1, 7.4% dysplasia; pattern 2, 9.1% dysplasia; pattern 3L, 0% dysplasia; pattern 3S, 8.3% dysplasia; pattern 4, 0% dysplasia, and pattern 5, 33.3% dysplasia). In addition, when we compared our ACF crypt patterns with the presence of hypercrinia, we found that as the complexity of the lesions increased, i.e., round to slit-like to gyriform pit patterns, the presence of hypercrinia also increased (P=0.03). This linear association was not found using Kudo's classification system (Table 3).

4. Immunohistochemistry Analysis

Staining patterns were analyzed with respect to the location of ACF, clinical groups, type of ACF mucosa (i.e., normal, hyperplastic, or dysplastic mucosal lining). During IHC analysis, adjacent ACF in a single case occasionally showed different staining patterns. However, the investigation of discordant results in the same patient was not our focus and we

https://doi.org/10.5217/ir.2018.16.1.116 • Intest Res 2018;16(1):116-125

Table 3. Comparison of Topographic and Histological Parameters between Kudo's System and Our Proposed Classification System for ACF

Parameter	Kudo's group							Our group			
	1	2	3S	3L	4	5	*P*-value	1	2	3	*P*-value
Hypercrinia	40.7	45.5	66.7	50.0	50.0	33.3	0.95	34.1	50.0	75.0	0.03
Mucosa							0.83				0.25
Normal	51.9	66.7	33.3	66.7	66.7	66.7		65.9	53.7	58.3	
Hyperplastic	40.7	24.2	66.7	25.0	33.3	0		29.5	35.7	25.0	
Dysplastic	7.4	9.1	0	8.3	0	33.3		4.5	10.7	16.6	
Laterality							0.61				0.22
Right	40.7	27.3	33.3	41.7	83.3	66.7		43.2	42.9	16.7	
Left	59.3	72.7	66.7	58.3	16.7	33.3		56.8	57.1	83.3	

Values are presented as percent.
ACF, aberrant crypt foci.

followed an "all or none" approach to interpretation.

1) Analysis of MMR Protein Expression

A total of 22 ACF cases showed negative staining for MLH1. Loss of staining was seen in 5 cases of ACF identified in controls without any pre-neoplastic link, 3 cases of ACF in controls with potentially pre-neoplastic disease, and in 14 cases of ACF in the context of colectomies with CRC (Table 4). Differential staining was also observed in a few cases, i.e., MLH1-positivity in normal crypts with negativity in the ACF (Fig. 1H). Only one case from the normal group (Bn) was found to have a loss of MSH2 staining (Fig. 1I), whereas none of the ACF in cases associated with pre-neoplastic diseases had a loss of MSH2 staining. A total of 13 ACF showed negative staining for MSH6 (Fig. 1J), of which 11 were in the CRC group A and 2 were in controls (group Bc) (Table 4). In colectomies with diseases without a known neoplastic link (Bn group), loss of MSH6 staining was not seen. All 13 ACF with MSH6-negative patterns were situated in the left colon. Only 3 cases in group A showed a loss of PMS2 immunohistochemical staining (2 cases in the left colon, 1 case in the right colon) (Fig. 1K). There was no correlation between the staining pattern for any of the markers and the mucosal histology of the ACF.

2) Marker of Cell Cycle-p53

A total of 56 ACF cases showed p53 nuclear positivity (Fig. 1L). p53 marker expression was found to be higher in the ACF associated with CRC (62.1%), than in the ACF in the other 2 groups (group Bn 41.2%, group Bc 36.4%; *P*=0.06) (Table 4). p53 positivity was noted in 43 of 71 (60.5%) left colonic ACF and in 13 of 34 (38.2%) right colonic ACF (*P*=0.03). Among these left colonic p53-positive cases, 30% had high ACF density and low-grade mucosal dysplasia. However, there was no correlation between high-grade mucosal histology and p53 expression when laterality was removed from the analysis.

5. *KRAS* Mutation Status

KRAS mutation was noted in 3 ACF cases out of the total 36 ACF analyzed for *KRAS* mutation. One *KRAS*-mutated ACF had a dysplastic mucosal lining, whereas the other 2 had hyperplastic linings. All 3 ACF were left-sided and had MSI, and one also showed p53 protein overexpression. In 3 ACF in which *KRAS* mutation was detected, this mutation was also identified in the corresponding tumor samples.

6. *BRAF V600E* Mutation Analysis by qPCR

BRAF V600E mutation was examined in 25 ACF and their corresponding tumor samples. None of the cases had the *V600E* mutation.

DISCUSSION

In our study, ACF-like lesions were identified in the grossly normal-looking colonic mucosa of patients with a variety of diseases including polyposis, adenomas and CRC, as well as in association with IBD, intestinal tuberculosis, inflammatory perforation, ischemia, and so forth.[9] We identified a greater number of ACF in the left colon than in the right colon. In colonic mucosa adjacent to CRC, the ACF identified showed increased number, density, size, and crypt multiplicity compared with those of the controls. In comparison to the ACF situated in right colon, the left colonic ACF had

Table 4. Molecular Markers and Mutational Analysis in Different Groups of ACF

IHC & molecular markers	ACF in control group Bn[a] (n=17) (*KRAS*: n=6)[c] (*BRAF*: n=2)[d]	ACF in control group Bc[b] (n=25) (*KRAS*: n=4)[c] (*BRAF*: n=5)[d]	ACF in CRC cases (n=65) (*KRAS*: n=26)[c] (*BRAF*: n=18)[d]	*P*-value
MSH2	1 (5.9)	0	3 (4.6)	0.55
MLH1	5 (29.4)	3 (13.6)	14 (20.9)	0.48
MSH6	0	2 (8.7)	11 (16.7)	0.14
PMS2	0	0	3 (4.6)	0.55
p53	7 (41.2)	8 (36.4)	41 (62.1)	0.06
BRAF[d]	0	0	0	NA
KRAS[c]	1 (2.8)	0	2 (5.6)	0.63

[a]Bn, controls in whom colectomy was performed for indications that do not have any association with colon carcinogenesis.
[b]Bc, controls in whom colectomy was performed for indications that have a known association with colon carcinogenesis.
[c]Analysis of *KRAS* mutation by high-resolution melting curve analysis was performed on select cases based on outcome of other markers studies.
[d]Analysis of *BRAF* mutation by real-time PCR was performed on randomly selected cases.
ACF, aberrant crypt foci; IHC, immunohistochemistry; CRC, colorectal carcinoma; NA, not applicable.

more risk factors, such as dysplasia and hypercrinia (increased goblet cell population). Hypercrinia was also more prevalent in colonic mucosa adjacent to foci of CRC and in the ACF with high crypt multiplicity (≥5/ACF). Our 3-tier ACF pit pattern classification showed good correlation with ACF histology and the presence of hypercrinia. The assessment of MSI was performed by the immunohistochemical method, and no statistically significant difference was noted between MMR protein negativity and ACF histology. Across the study groups, although the number of IHC-negative cases (mutated/methylated) was found to be less, there was a slight predominance of the loss of microsatellite markers in ACF associated with CRC (group A). There was significantly greater p53 protein overexpression in both the left-sided ACF and the ACF associated with CRC. The *KRAS* gene mutation was found more frequently in the left-sided ACF, one of which showed histological dysplasia, and there was no association between the *KRAS* gene mutation and hypercrinia. The *BRAF* V600E mutation was not identified in any of the ACF or corresponding tumor samples that were examined, irrespective of laterality.

A previously published study employing confocal chromoendoscopy that was performed on 861 subjects (normal subjects, adenoma cases, and CRC cases), showed an increasing prevalence of ACF in cases of CRC compared to that in the adenomas and in normal colonic mucosa, suggesting that ACF may be an early surrogate microscopic marker for human colon carcinogenesis.[13] In a study published by Roncucci et al.,[14] greater ACF density was found in diseases, such as familial adenomatous polyposis and CRC than in benign colonic diseases, with a positive ACF density gradient from the proximal to the distal colon. Our results were in accordance with these studies. A topographic classification system that can triage the ACF according to their risk of developing CRC in future has been lacking. Based on a large endoscopic study on crypt patterns incorporating normal colonic mucosa, polyps, adenomas, and carcinomas, a system of crypt pattern classification was described by Kudo et al.[10] According to Kudo's system, the slit-like pattern, gyriform pattern, and non-structural pits were categorized as high-risk crypts, whereas the rounded crypts were the most innocuous. In the study by Roncucci et al.,[15] the round luminal pattern was determined to be the benign type, whereas the slit-like ACF were commonly associated with histologic dysplasia. In our study, the round/oval ACF pit pattern was the most common, whereas the ACF with gyriform and slit-like pit patterns had a more dysplastic histology, thereby qualifying as high-risk ACF subtypes. However, Kudo's classification system was formulated using a large number of crypt patterns and is highly acclaimed; our pit pattern was formulated based on our topographic findings in human mucosal ACF only. Hence, we suggest that our morphological classification method be used solely for triaging ACF and not for other colonic lesions.

Few studies have investigated ACF in human colonic mucosa in terms of MMR protein expression. Although IHC cannot differentiate between a true MMR gene mutation and epigenetic silencing, the utility of IHC to diagnose MSI in CRC has been previously validated by molecular methods. The issue of the interpretation of IHC results as positive or negative has been variously addressed, though predominantly in tumors. To date, no study has examined

https://doi.org/10.5217/ir.2018.16.1.116 • Intest Res 2018;16(1):116-125

the expression of MMR proteins in ACF by the IHC method. However, MMR gene status has been studied in ACF by molecular methods.[16] Therefore, our IHC interpretation is subject to validation using molecular methods. While strong diffuse staining of MMR proteins in tumor tissue implies intact MMR gene expression, focal weak staining or the loss of staining in tumor tissue imply mutated MMR genes or the epigenetic silencing of MMR genes.[17] The interpretation of MMR staining in ACF remains unclear. Moreover, there is a wide variation in the results reported in the published literature regarding MMR gene expression. In some studies, loss of expression of these proteins was found in only 2% of tumors,[18,19] whereas others have shown MLH1 inactivation through epigenetic silencing in up to 90% of sporadic MSI+ cancers.[20-22] This epigenetic alteration is speculated to be an early event in sporadic CRC that arises through serrated, non-dysplastic adenomas.[22,23] Greenspan et al.[24] identified hMLH1 promoter hypermethylation in 8 of 39 ACF (21%), with no correlation found between hMLH1 promoter hypermethylation and MSI. In this study, we identified MLH1 protein loss in 20% of ACF. In 3 of our ACF, the complete loss of all MMR markers was observed. Although we identified differential MMR protein expression patterns in some ACF, we adopted an all-or-none approach in which ACF with diffuse expression were considered MSS, whereas ACF with partial or no stain expression were considered microsatellite instable lesions. In a study by Cheng and Lai,[16] the authors identified differential MMR gene expression patterns in various ACF found in the colonic mucosa of a single patient. While some of the ACF had MSI, the others showed the MSS pattern. Similarly, no correlation between MMR protein expression and ACF histology was found in the present study.[16]

Although the *TP53* mutation has been considered a late event in carcinogenesis,[11] almost 30% of the left-sided ACF had low-grade dysplasia with increased p53 protein expression. Whether all of these dysplastic ACF will eventually progress to adenomas or not, and what is the estimated timeframe of such a progression are not conclusively known. Yamashita et al.[25] observed more frequent *TP53* mutations in left colonic ACF than in right colonic ACF, and increased p53 positivity in left colonic ACF was found in our study as well (60.5% vs. 38.2%, P=0.03).[11]

The serrated pathway is implicated with sessile serrated adenomas and polyps in the right colon and is characterized by a distinct molecular signature involving mutations in mismatch repair (*MMR*) genes and in the *BRAF* gene. In a recent study published by Inoue et al.,[8] serrated polyps identified in the right colon were associated with ACF found in the vicinity, both of which showed mutation of the *BRAF* gene and gene promoter methylation. In a series of 55 cases of ACF, Rosenberg et al.[26] reported *BRAF V600E* mutation in 10 of 16 serrated lesions, as compared to that in only 1 of 33 non-serrated lesions (P=0.001). *KRAS* mutation was detected in 3 of 16 serrated ACF, in comparison to that in 14 of 33 non-serrated ACF lesions. The authors also found that 11% of the hyperplastic ACF (5/45) and 25% (1/4) of the dysplastic ACF were the MSI-H type. MSI was not associated with the *BRAF* mutation in ACF, indicating that MSI was a late event in the serrated polyp pathway. Beach et al.[27] also showed that *BRAF* mutation in ACF was associated with hyperplastic polyposis. In our study, no serrated pattern was noted in any of the ACF identified. None of our ACF showed *BRAF* mutation, whereas 3 ACF showed *KRAS* mutation. Loss of MMR proteins was not significantly different between the left and right colonic ACF in the index study.

To our knowledge, the presence of hypercrinia in ACF has not been previously described, and the term has mainly been used in relation to crypt changes in IBD, especially CD.[28] Hypercrinia was identified frequently in left colonic ACF in our study. ACF with low-grade dysplasia also showed hypercrinia. These results all suggest that hypercrinia can be used as a histological marker for high-risk ACF. The potential link between excessive mucin production and the pathogenesis of these lesions remain to be investigated further.

Given that ACF-like lesions can be identified *in vivo* using the magnified chromoendoscopy technique, herein, we aimed to create a study design that would closely mimic a magnified chromoendoscopic view. Based on the current knowledge, chromoendoscopic screening of the whole colon in high-risk subjects is not yet indicated. Therefore, we needed to assess the presence of any topographic, histological, and genetic differences in ACF found in human colectomies belonging to different clinical groups. Based on our findings, it is apparent that there are no indisputable criteria that can accurately differentiate the ACF found in these groups. On multivariate analysis, only p53 protein overexpression was found to be significantly associated with high-risk ACF. The findings may indicate that any ACF in human colon should not be discounted during chromoendoscopy. There are several limitations in this study. First, an elaborative study of genetic change was not performed. We undertook this work as a pilot study and further detailed genetic workups are being performed. Second, we did not validate the MMR protein expression pattern with *MMR* gene amplification. In conclusion, no significant topographic, histological, and genetic differences exist in ACF identified in different clinical

settings. High-risk ACF appear mostly in the left colon and show increased density, crypt multiplicity, hypercrinia, and p53 accumulation. The topographic pit pattern described in this study is simple to remember and can predict a greater likelihood of histological hypercrinia and dysplasia.

SUPPORTING INFORMATION

1. Aberrant crypt foci (ACF) are a cluster of dilated and occasionally distorted crypts in comparison to the surrounding area, with a large pericryptal zone. The thick epithelial lining stains darker with methylene blue as compared to normal crypts. The luminal opening is 2 to 3 times larger than normal and the crypt pit pattern can be variable. In some cases, ACF were seen as a single aberrant crypt and not as a cluster.

2. ACF density refers to the number of ACF per square centimeter of mucosal surface.

3. Elevated ACF implies that the luminal openings lie above the level of the adjacent normal mucosa when viewed end-on as in magnified chromoendoscopy or as in our case under 40× magnification microscopy. In contrast, flat ACF have luminal openings at the same level as that of adjacent normal mucosa.

4. Hyperplastic ACF refers to ACF with hyperplastic epithelial lining and no dysplasia on histology.

5. Dysplastic ACF (microadenoma) show nuclear stratification, enlargement, hyperchromasia, loss of polarity, prominent nucleoli, and irregular outline on histology. We divided dysplastic ACF into low-grade and high-grade types based on the standard definitions of dysplasia used in pathology.

6. Hypercrinia refers to an increased number of goblet cells with near extinction of absorptive cells and increased mucin production on light microscopy.

7. Kudo's classification is a 5-tier endoscopic classification system (1, roundish; 2, stellar or papillary; 3S, small-roundish or tubular; 3L, large-roundish or tubular; 4, branch-like or gyrus; and 5, non-structured pits) to identify the various morphological appearances of colonic crypts described with magnifying endoscopes after methylene blue staining of the mucosa.10

8. Our proposed topographic classification system has been devised to identify ACF after methylene blue staining and can be applied to chromoendoscopy as well. It is a 3-tier system that describes round, slit-like, and gyriform pits (Fig. 1A-C).

FINANCIAL SUPPORT

This study was partly supported by the Department of Biotechnology, Government of India (grant number: 6242-P38/RGCB/PMD/DBT/PSNJ/2015).

CONFLICT OF INTEREST

No potential conflict of interest relevant to this article was reported.

AUTHOR CONTRIBUTION

S.G., B.G., S.D.G., and P.D. are responsible for designing the study, doing all experiments, analysing data and proof reading of the manuscript. P.V., S.G., and P.D. are responsible for molecular tests performed. S.V. is responsible for statistical analysis. S.P. and N.R.D. are responsible for management of the patients and for surgical excision of the colon specimens. P.D. is the overall guarantor of this article.

REFERENCES

1. Pathy S, Lambert R, Sauvaget C, Sankaranarayanan R. The incidence and survival rates of colorectal cancer in India remain low compared with rising rates in East Asia. Dis Colon Rectum 2012;55:900-906.
2. Indian Council of Medical Research. ICMR Bulletin. New Delhi, India: Indian Council of Medical Research, 2010.
3. Mohandas KM. Colorectal cancer in India: controversies, enigmas and primary prevention. Indian J Gastroenterol 2011;30:3-6.
4. Luo Y, Yu M, Grady WM. Field cancerization in the colon: a role for aberrant DNA methylation? Gastroenterol Rep (Oxf) 2014;2:16-20.
5. Bird RP. Observation and quantification of aberrant crypts in the murine colon treated with a colon carcinogen: preliminary findings. Cancer Lett 1987;37:147-151.
6. Caderni G, Femia AP, Giannini A, et al. Identification of mucin-depleted foci in the unsectioned colon of azoxymethane-treated rats: correlation with carcinogenesis. Cancer Res 2003;63:2388-2392.
7. Takayama T, Ohi M, Hayashi T, et al. Analysis of K-ras, APC, and beta-catenin in aberrant crypt foci in sporadic adenoma, cancer, and familial adenomatous polyposis. Gastroenterology 2001;121:599-611.

8. Inoue A, Okamoto K, Fujino Y, et al. B-RAF mutation and accumulated gene methylation in aberrant crypt foci (ACF), sessile serrated adenoma/polyp (SSA/P) and cancer in SSA/P. Br J Cancer 2015;112:403-412.
9. Gupta B, Das P, Ghosh S, et al. Identification of high-risk aberrant crypt foci and mucin-depleted foci in the human colon with study of colon cancer stem cell markers. Clin Colorectal Cancer 2017;16:204-213.
10. Kudo S, Hirota S, Nakajima T, et al. Colorectal tumours and pit pattern. J Clin Pathol 1994;47:880-885.
11. Das P, Jain D, Vaiphei K, Wig JD. Abberant crypt foci–importance in colorectal carcinogenesis and expression of p53 and mdm2: a changing concept. Dig Dis Sci 2008;53:2183-2188.
12. Benlloch S, Payá A, Alenda C, et al. Detection of BRAF V600E mutation in colorectal cancer: comparison of automatic sequencing and real-time chemistry methodology. J Mol Diagn 2006;8:540-543.
13. Sakai E, Takahashi H, Kato S, et al. Investigation of the prevalence and number of aberrant crypt foci associated with human colorectal neoplasm. Cancer Epidemiol Biomarkers Prev 2011;20:1918-1924.
14. Roncucci L, Pedroni M, Vaccina F, Benatti P, Marzona L, De Pol A. Aberrant crypt foci in colorectal carcinogenesis: cell and crypt dynamics. Cell Prolif 2000;33:1-18.
15. Roncucci L, Medline A, Bruce WR. Classification of aberrant crypt foci and microadenomas in human colon. Cancer Epidemiol Biomarkers Prev 1991;1:57-60.
16. Cheng L, Lai MD. Aberrant crypt foci as microscopic precursors of colorectal cancer. World J Gastroenterol 2003;9:2642-2649.
17. de Jong AE, van Puijenbroek M, Hendriks Y, et al. Microsatellite instability, immunohistochemistry, and additional PMS2 staining in suspected hereditary nonpolyposis colorectal cancer. Clin Cancer Res 2004;10:972-980.
18. Shia J. Immunohistochemistry versus microsatellite instability testing for screening colorectal cancer patients at risk for hereditary nonpolyposis colorectal cancer syndrome. Part I. The utility of immunohistochemistry. J Mol Diagn 2008;10:293-300.
19. Kim H, Jen J, Vogelstein B, Hamilton SR. Clinical and pathological characteristics of sporadic colorectal carcinomas with DNA replication errors in microsatellite sequences. Am J Pathol 1994;145:148-156.
20. Young J, Simms LA, Biden KG, et al. Features of colorectal cancers with high-level microsatellite instability occurring in familial and sporadic settings: parallel pathways of tumorigenesis. Am J Pathol 2001;159:2107-2116.
21. Deng G, Chen A, Hong J, Chae HS, Kim YS. Methylation of CpG in a small region of the hMLH1 promoter invariably correlates with the absence of gene expression. Cancer Res 1999;59:2029-2033.
22. Giovannucci E, Ogino S. DNA methylation, field effects, and colorectal cancer. J Natl Cancer Inst 2005;97:1317-1319.
23. Jass JR, Whitehall VL, Young J, Leggett BA. Emerging concepts in colorectal neoplasia. Gastroenterology 2002;123:862-876.
24. Greenspan EJ, Cyr JL, Pleau DC, et al. Microsatellite instability in aberrant crypt foci from patients without concurrent colon cancer. Carcinogenesis 2007;28:769-776.
25. Yamashita N, Minamoto T, Ochiai A, Onda M, Esumi H. Frequent and characteristic K-ras activation and absence of p53 protein accumulation in aberrant crypt foci of the colon. Gastroenterology 1995;108:434-440.
26. Rosenberg DW, Yang S, Pleau DC, et al. Mutations in BRAF and KRAS differentially distinguish serrated versus non-serrated hyperplastic aberrant crypt foci in humans. Cancer Res 2007;67:3551-3554.
27. Beach R, Chan AO, Wu TT, et al. BRAF mutations in aberrant crypt foci and hyperplastic polyposis. Am J Pathol 2005;166:1069-1075.
28. Geboes K, El-Zine MY, Dalle I, El-Haddad S, Rutgeerts P, Van Eyken P. Tenascin and strictures in inflammatory bowel disease: an immunohistochemical study. Int J Surg Pathol 2001;9:281-286.